doi:10.1111/evo.12671

The fitness effect of mutations across environments: Fisher's geometrical model with multiple optima

Guillaume Martin[1,2] and Thomas Lenormand[3]

[1] *Institut des Sciences de l'Evolution de Montpellier, UMR CNRS-UM II 5554, Université Montpellier II, 34 095 Montpellier cedex 5, France*

[2] *E-mail: guillaume.martin@univ-montp2.fr*

[3] *UMR 5175 CEFE, CNRS – Université Montpellier – Université P. Valéry, EPHE, 1919 route de Mende 34293 Montpellier Cedex 5, France*

Received May 21, 2014
Accepted April 7, 2015

When are mutations beneficial in one environment and deleterious in another? More generally, what is the relationship between mutation effects across environments? These questions are crucial to predict adaptation in heterogeneous conditions in a broad sense. Empirical evidence documents various patterns of fitness effects across environments but we still lack a framework to analyze these multivariate data. In this article, we extend Fisher's geometrical model to multiple environments determining distinct peaks. We derive the fitness distribution, in one environment, among mutants with a given fitness in another and the bivariate distribution of random mutants' fitnesses across two or more environments. The geometry of the phenotype-fitness landscape is naturally interpreted in terms of fitness trade-offs between environments. These results may be used to fit/predict empirical distributions or to predict the pattern of adaptation across heterogeneous conditions. As an example, we derive the genomic rate of substitution and of adaptation in a metapopulation divided into two distinct habitats in a high migration regime and show that they depend critically on the geometry of the phenotype-fitness landscape.

KEY WORDS: **Adaptation, evolution, fitness, life-history, models/simulations, mutations, pleiotropy.**

Mutations are often characterized as beneficial, neutral or deleterious. This division suggests an absolute and fixed property of mutations, each of these classes being studied separately. However, this view dissolves even with "a small tincture of ecological reality" (Bell 2008). In the simplest case of two environments, a mutation may be beneficial in both environments (+|+), deleterious in both (–|–), or exhibit antagonistic effects (+|– or –|+). Along an ecological gradient or across multiple environments, the number of possible combinations explodes, questioning a simple classification. Here, the environment may be taken in its traditional ecological conception, or it may encompass a diversity of genetic and physiological "environments" (e.g., across sexes, ploidy levels, stages, or ages etc.): for example sex-specific mutation fitness effects have been documented in *Drosophila melanogaster* (Wang et al. 2009; Innocenti and Morrow 2010). The pattern of variation in mutation effects on fitness across multiple "environments" is central to any evolutionary process involving adaptation to heterogeneous conditions in this broad sense; including the evolution of specialization (Kassen 2002; Lenormand 2012) and of species niche and range (Polechova et al. 2009), but also the evolution of senescence (Williams 1957; Moorad and Hall 2009, Cotto and Ronce (2014)), sexual conflict (Connallon and Clark 2014) or life cycles (Immler et al. 2012). It has also important evolutionary implications for resistance management where most strategies (Lenormand and Raymond 1998; R.E.X. Consortium 2010) rely on the assumption that (+|?) mutations are in fact (+|–) mutations. That is, resistance genes to pesticide, herbicide, antibiotics, etc. are most often assumed to exhibit a "fitness cost."

Relatively few studies have investigated the distribution of the fitness effects of mutations (hereafter "DFE") in multiple

EVOLUTION
INTERNATIONAL JOURNAL OF ORGANIC EVOLUTION

environments (see below). These studies typically involve generating a collection of "random" mutants and measuring their fitness relative to their unmutated ancestor, across conditions. Such studies (summarized below) can be classified according to the method used to obtain mutants. A first option is to artificially engineer random single mutants. This was applied to measure the DFE across different abiotic conditions: in *E. coli* with random transposon inserts (Remold and Lenski 2001), with visible phenotype mutations introgressed into *Drosophila melanogaster* lines (Wang et al. 2009), and in *Saccharomyces cerevisiae,* with single nucleotide substitutions on the *hsp90* gene (Hietpas et al. 2013) or with single gene deletions (Jasnos et al. 2008). It was also applied to measure the DFE across biotic conditions (alternative hosts), using random single nucleotide substitutions, in a plant virus (Lalic et al. 2011) and a bacteriophage (Vale et al. 2012). A more common alternative is to generate mutant lines via mutation-accumulation experiments where drift is maximized: here, spontaneous mutations accumulate in each subline, but their number is unknown (reviewed in, e.g., Fry and Heinsohn 2002; Korona 2004; Martin and Lenormand 2006a; Agrawal and Whitlock 2010). In all these experiments, the mutants are sampled independently of their fitness effect: we note them (?|?), where the question marks indicate that sampling is independent of fitness in either environment. In practice, selection cannot be fully avoided in these protocols (for instance lethal mutations are typically lost), but the bias is expected to be minor for the bulk of mild-effect mutations (Gordo and Dionisio 2005). A third option is to deliberately select ("screen") a subset of beneficial mutants in one environment, and measure their fitness in alternative environments. We note them (+|?), accordingly. The screening can be done directly on a selective medium where the wild-type genotype does not grow: antibiotics for bacteria, selective host for viruses etc. (Kassen and Bataillon 2006; MacLean et al. 2010; Bataillon et al. 2011; Trindade et al. 2012). Beneficial mutants can also be obtained using experimental evolution, and a posteriori identification by sequencing (e.g., Wong et al. 2012) or using genetic marker frequency dynamics (Ostrowski et al. 2005). In these studies, (+|?) mutations spanned the entire range of possible effects from (+|–) to (+|+) (Kassen and Bataillon 2006). Indeed, as often pointed out (e.g., Fry 1993; Fry 1996), adaptation to particular conditions need not systematically impede adaptation to alternative conditions (be "costly"), unless they arise in a genotype already well adapted to these latter conditions.

Overall, mutation effects across environments have been empirically investigated in many ways, but the corresponding theory is still unable to make sense of all the information in the available datasets. The classic framework to model heterogeneous environments (and life history trade-offs in general), introduced by Levins (1968), assumes that fitness is a concave (typically Gaussian or quadratic) function $w(z)$ of some underlying trait or set of traits z. Distinct environments determine distinct optima for these traits and possibly distinct shapes of the fitness function. This approach has been used to investigate adaptation to heterogeneous conditions, for example in cline models (Slatkin 1978), in species range models (e.g., Kirkpatrick and Barton 1997; Polechova et al. 2009; Duputie et al. 2012), or moving optimum models (e.g., Kopp and Matuszewski 2014). In these studies, a quantitative genetics model is used to approximate large polymorphic populations under weak selection, where both drift and the dynamics of genetic covariances among traits can be ignored. An alternative regime is when selection is strong and drift is important so that adaptive dynamics are better analyzed as a succession of stochastic fixations. This approach requires a prediction of the multivariate DFE across environments, and how it evolves as the population adapts. Such prediction is also central to fit and take full advantage of the multivariate nature of the empirical DFEs across environments detailed above.

In single environments, Fisher's (1930) geometrical model (hereafter "FGM") has proved useful to undertake the leap from quantitative genetics models to stochastic fixation models (reviewed in Orr 2005; McCandlish and Stoltzfus 2014). The FGM assumes a Gaussian fitness function and (typically) a Gaussian distribution of mutation effects on phenotype, and predicts the DFE in a given environment, that notably depends on the level of adaptation of the wild type to this environment (Martin and Lenormand 2006b). From this initial use in theories of adaptation, the FGM can also serve as a null model to fit and interpret empirical DFEs. Indeed, this model was shown to capture the DFE of single mutants (Martin and Lenormand 2006b), of epistasis (Martin et al. 2007) or of dominance (Manna et al 2011). With respect to environmental effects, which is our focus here, (Martin and Lenormand 2006a) showed that mutation accumulation data was consistent with a concave, nearly Gaussian phenotype-fitness function with constant shape and varying optima across environments. Other studies tested the FGM using engineered random (?|?) mutations (Vale et al. 2012; Hietpas et al. 2013), compensatory (+|?) (Sousa et al. 2011; Perfeito et al. 2014), or screened (+|?) mutations (Trindade et al. 2012). Whether (+|?) mutations should be analyzed as truly random (?|?) is an unsettled matter, by lack of a theory of the DFE of different types of mutants in different environments.

Overall, a full description of the multivariate DFE across environments would be useful on two grounds. First, it would provide a null model to study the various types of empirical datasets described above (and others to come). Second it would allow extending theories of adaptation to heterogeneous environments when polymorphism is limited and stochastic fixations form the fuel of adaptation. Using the FGM to do so seems a natural option, given its link to theories of adaptation across environments and its ability to capture patterns so far.

Table 1. Notations.

Notation	Formulae	Denotation/biological meaning
S_i	Eqs.(1–2)	Fitness effect of a random mutation in environment i: selection coefficient relative to the unmutated ancestor.
$n(\eta)$	$\eta = n/2$	n : dimensionality (number of traits under selection) η : shape parameter of the (gamma distributed) DFE at the optimum.
$\bar{s}$	$\bar{s} = -E(S_i) = -E(S_j)$	Mean fitness effect of random mutations in any environment.
λ	$\bar{s} = \eta\lambda$	Mutational variance per trait among random mutations (scales the mean fitness effect of mutations).
s_o^i	$s_o^i = \log(W_{max}/W_i)$	Fitness distance to the optimum in environment i.
ε_i	$\varepsilon_i = s_o^i/\bar{s}$	scaled Fitness distance to the optimum.
ν	$\nu^2 = \varepsilon_j/\varepsilon_i$	Relative distance to each optimum (j vs. i).
U_i	$U_i = \frac{\mathbf{z}_i.\mathbf{dz}}{\|\mathbf{z}_i\|.\|\mathbf{dz}\|}$	Cosine of the angle between a mutant phenotypic effect **dz** and the direction to the optimum in i ($\mathbf{z}_i$), from the ancestor.
ρ	$\rho = \frac{\mathbf{z}_i.\mathbf{z}_j}{\|\mathbf{z}_i\|.\|\mathbf{z}_j\|}$	Cosine of the angle between directions to each optimum (i and j), from the ancestor.
ρ_{ij}	$cor\left(S_i, S_j\right)$, equation (6)	Fitness correlation among random mutants, between environments i and j.
$f_S(s, n, \lambda, s_o)$	Equation (3)	DFE among random mutations, with a parent lying at a distance s_o in n dimensions and with a mean phenotypic step per trait λ.
$S_j \vert S_i = s$		Fitness effect in environment j, conditional on mutations having fitness effect s in environment i.
γ^*	$\gamma^* = \|\mathbf{dz}\|^2/\|\mathbf{z}_i\|^2$	Mutant effect size (scaled by the distance to the optimum in environment i).

Real random variables are indicated by uppercase letters (e.g., X) and constants and particular realizations (e.g., $X = x \in \mathbb{R}^+$) with lowercase letters. Random vectors are indicated by lowercase boldface. The probability density function (pdf) of a random variable X (resp. set of variables X_i, X_j) is denoted $f_X(x)$ (resp. $f_{X_i,X_j}(x_i, x_j)$). Similar notations are used for the moment generating functions (mgf $M_X(z)$ or $M_{X_i,X_j}(z_i, z_j)$ defined on $z \in \mathbb{R}^-$ or $(z_i, z_j) \in \mathbb{R}^- \times \mathbb{R}^-$) or cumulant generating functions (mgf $C_X(z)$ or $C_{X_i,X_j}(z_i, z_j)$ defined on the same sets.

This paper aims at deriving this multivariate theory and illustrating its application. More precisely, we consider a mutation that has effect S_i (resp. S_j) in environment i (resp. j), relative to its nonmutated ancestor. We derive the joint distribution of S_i and S_j among random mutations ((?|?) mutations), under the isotropic FGM, that is when selection and mutation affect each trait identically and independently (absence of genetic covariance between traits). We then provide the conditional distribution $S_j|S_i$ or of S_j in environment j, for the subset of mutants with given effect S_i in environment i. Finally, we apply our results to derive a genomic rate of adaptation in a metapopulation with two habitats.

Model

We start from the isotropic FGM and extend it to multiple environments. We consider the minimal extension where each environment determines a distinct phenotypic optimum, while other parameters of the model remain unchanged across environments (number of traits n, strength of selection and mutational variance). The potential effect of relaxing some of these assumptions is discussed and studied in simulations of less simplified scenarios.

Table 1 summarizes the main notations used in the model; most derivations can be checked in the supplementary Mathematica ® notebook file 1 (Wolfram Research 2012) and figures and simulations can be generated through the supplementary notebook file 2. Let us start by briefly presenting the case of a single environment, to introduce notations and summarize results in this situation.

FITNESS EFFECT OF MUTANTS IN A SINGLE ENVIRONMENT

Definitions

Let $\mathbf{z}$ be the n-dimensional vector describing a given phenotype, assumed constant in all environments (no plasticity). We assume that the fitness of a phenotype $\mathbf{z}$, in any environment i, is a multivariate Gaussian function $W_i(\mathbf{z})$. The vector pointing from the nonmutated wild-type phenotype to the optimum in environment i is denoted $\mathbf{z}_i$, so the wild-type fitness in i is $W_i(-\mathbf{z}_i)$. Mutations generate an isotropic multivariate normal displacement **dz** around the wild-type phenotype : $\mathbf{dz} \sim N(0, \lambda\mathbf{I}_n)$, where $\mathbf{I}_n$ is the identity matrix in n dimensions and λ is a scaling factor. In environment i, the selection coefficient of a mutation with effect **dz**, S_i (**dz**), is defined as the log-fitness of the mutant phenotype minus that of the wild type. This gives the exact selection coefficient for a continuous time model (overlapping generations) and approximates it for weak selection in discrete time models (Rice 2004). We have

$$S_i\left(\mathbf{dz}\right) = \log\left(\frac{W_i\left(-\mathbf{z}_i + \mathbf{dz}\right)}{W_i\left(-\mathbf{z}_i\right)}\right) = \mathbf{z}_i^T.\mathbf{dz} - \frac{\mathbf{dz}^T.\mathbf{dz}}{2}, \quad (1)$$

where ^{T} denotes transposition. A key simplification occurs in this isotropic model because the norm of the mutant vector **dz** is independent of its direction, which itself is uniformly distributed over all possible directions in n dimensions. We can therefore express equation (1) in terms of independently distributed polar coordinates: this provides a stochastic representation of the random variable S_i. We define $z_i = \| \mathbf{z}_i \|$ as the distance to the optimum in i and the (random) polar coordinates: $R = \| \mathbf{dz} \|$, norm of **dz** and θ_i, angle between the direction of the mutation and the direction to the optimum from the wild type (hereafter "optimal direction"). We also define $U_i = \cos(\theta_i)$ the (random) cosine of this angle with the optimal direction, so that $\mathbf{dz}.\mathbf{z}_i = Rz_i \cos(\theta_i)$ and equation (1) simplifies to

$$S_i\left(R, \theta_i\right) = Rz_iU_i - \frac{R^2}{2}. \quad (2)$$

The distribution of $S_i$is referred to as the distribution of fitness effects (DFE), in a given environment.

Moments and empirical parameterization

One difficulty with landscape models in general (both genetic and phenotypic) is empirical parameterization. With FGM, it is possible to express the landscape parameters exclusively in terms of fitness effects, that are in principle measurable (Martin and Lenormand 2006b). The isotropic model can be fully specified from (i) the degree of maladaptation of the wild type in environment i, and (ii) the mean and variance of mutation fitness effects relative to this wild type in that environment. The degree of maladaptation of the wild type can be measured as the selection coefficient of a perfectly adapted genotype ($\mathbf{z} = 0$) relative to the wild type : $s_o^i = \log(W_i(0)/W_i(-\mathbf{z}_i)) = z_i^2/2$, or equivalently $z_i = \sqrt{2s_o^i}$. It is also the maximum possible selective effect in that environment, corresponding to a mutation $\mathbf{dz} = \mathbf{z}_i$ positioning the mutant exactly at the optimum. For example, s_o^i may be estimated by performing long term experimental evolution in that environment. We define the absolute mean effect of mutations $|E(S_i)| = \bar{s}$ and $\varepsilon_i \equiv s_o^i/\bar{s}$, a measure of the distance to the optimum in environment i, scaled by $\bar{s}$. This mean effect $\bar{s}$ is constant across environments when those environments only determine the position of the phenotypic optimum (Martin and Lenormand 2006b). The remaining parameters in the model are the scale λ and dimensionality n, they can be obtained from an empirical DFE, by fitting its first moments or the full distribution (Martin and Lenormand 2006b), described below.

Distribution of effects

The probability density function (pdf) of the DFE in the isotropic FGM is fully determined by (n, λ, s_o^i) and can be derived exactly

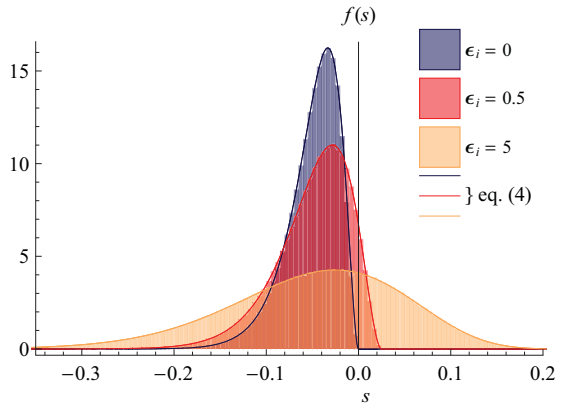

Figure 1. Univariate distribution of fitness effects (DFE). The histograms show the DFE among 10^6 simulated random mutants in the isotropic Fisher's model, for different distances to the optimum (ε_i, see legend). The wild-type position in n-dimensions was set as $\mathbf{z}_i = \sqrt{2\varepsilon_i}\bar{s}\mathbf{u}_1$, where $\mathbf{u}_1$ is the unit vector along the 1st dimension. Each mutant was obtained by drawing a multivariate Gaussian deviate $\mathbf{dz} \sim N(0, \lambda \mathbf{I}_n)$, and its fitness effect was computed as $S(\mathbf{z}_i, \mathbf{dz})$ using equation (1). The landscape parameters are $n = 6$, $\bar{s} = 0.05$. The lines show the corresponding theoretical probability density function $f_S(s, n, \lambda, s_o^i)$ in equation (3).

(see also Martin 2014; McCandlish et al. 2014). Its stochastic representation (Supp. Online Text Section 1) and pdf $f_S(s, n, \lambda, s_o^i)$ are

$$S_i \sim s_o^i - \frac{\lambda}{2}\chi_n^2\left(\frac{2s_o^i}{\lambda}\right)$$

$$f_S\left(s, n, \lambda, s_o^i\right) = \frac{2}{\lambda} f_{\chi_n^2}\left(\frac{2\left(s_o^i - s\right)}{\lambda}, \frac{2s_o^i}{\lambda}\right), \quad (3)$$

where $\chi_n^2(c)$ is a noncentral chi-square deviate with n degrees of freedom and noncentrality $c > 0$ and $f_{\chi_n^2}(x, c)$is its corresponding pdf at $x \in \mathrm{R}^+$. This distribution encompasses both beneficial and deleterious mutations and depends on only three parameters (n, λ, s_o^i). It is illustrated on Figure 1, for various levels of maladaptation s_o^i, with exact simulations of equation (1), as a check of the simulation code (the result being exact, perfect agreement is expected). Close to the optimum ($\mathbf{z}_i \to 0$), all mutations are deleterious and follow a negative gamma distribution: $S_i \sim -\Gamma(n/2, \lambda)$, with shape $n/2$ and scale λ, as already pointed out in (Martin and Lenormand 2006b). The exact DFE above is not more parameterized than previously proposed approximations for this model (e.g., displaced gamma in Martin and Lenormand 2006b), so it should be used instead when possible.

FITNESS EFFECT OF RANDOM MUTANTS ACROSS ENVIRONMENTS

We want to compute the effects of a given mutation, relative to its nonmutant parent (wild type), in two environments, only differing by the position of their optimum. In the following, we label these

two environments i and j: we wish to derive the joint distribution of (S_i, S_j), which, from equation (2), depends on the distribution of the corresponding $(R, U_i = cos(\theta_i))$ and $\left(R, U_j = cos(\theta_j)\right)$, in each environment. The mutant size R is the same in all environments; in the isotropic model, it is independent of the angles (θ_i, θ_j) between the mutant and optimal directions (from reference to optimum) in each environment. The squared mutant size, R^2, is distributed as twice the DFE at the optimum, as defined above (eq. (3)). Therefore, R^2 is gamma distributed (R is Nagakami distributed): $R^2 \sim \Gamma(n/2, 2\lambda)$. However, in order to obtain the full bivariate distribution of (S_i, S_j), we also need to derive the joint distribution of (U_i, U_j).

Angle distribution

The covariance between angles will depend on the angle between optimal directions in each environment. Intuitively, one expects that these angles will covary positively if the two optima are in roughly the same direction from the reference phenotype, and negatively if they are in opposite directions. In Supp. Online Text Section 1, we confirm this intuition and obtain the exact joint distribution of (U_i, U_j), using a result from n-dimensional geometrical probability (Lemma 2 of Cambanis et al. 1981). This lemma describes the distribution of the projection of a random vector with arbitrary spherically symmetric distribution onto a subspace of lower dimension (the approach is illustrated in Fig. S1). Let $\rho = \cos\left(\psi_{ij}\right) = \mathbf{z}_i.\mathbf{z}_j/(z_i z_j)$ be the cosine of the angle between optimal directions in each environment (i and j). The distribution of $\left(U_i = \cos\left(\theta_i\right), U_j = \cos\left(\theta_j\right)\right)$ has bivariate pdf:

$$f_{U_i,U_j}\left(u_i, u_j\right) = \frac{n/2-1}{\sqrt{1-\rho^2}\pi}\left(1 - \frac{\left(u_i^2 + u_j^2 - 2\rho u_i u_j\right)}{1-\rho^2}\right)^{n/2-2}, \tag{4}$$

when $0 < u_i^2 + u_j^2 - 2\rho u_i u_j < 1 - \rho^2$ and zero otherwise. This distribution has correlation $cor\left(U_i, U_j\right) = \rho$ (see also Connallon and Clark 2014). Its agreement with stochastic simulations is illustrated in Fig. S2. When the two optimal directions are orthogonal ($\psi_{ij} = \pi/2 \text{or} -\pi/2$), then $\rho = 0$ and U_j and U_i are uncorrelated. By contrast, when the reference and the two optima are aligned, the angle is $\psi_{ij} = 0$ or $\psi_{ij} = \pi$, then $\rho = 1$ (resp. $\rho = -1$), so that U_i and U_j are fully correlated. Note that equation (4) is valid for any spherically symmetric distribution, so our model could be extended to any such distribution for $\mathbf{dz}$ (i.e., not only the multivariate Gaussian), using the corresponding distribution for R. The marginal distribution $f_{U_i}(u_i)$ of $U_i = \cos(\theta_i)$ in any environment, can be retrieved directly from (Lemma 2 of Cambanis et al. 1981) or by integrating the bivariate pdf in equation (4) over the domain of U_j. This retrieves the known result: $f_{U_i}(u_i) \propto (1-u_i^2)^{(n-3)/2}$ with a proper scaling constant (see Supp. Online Text Section 1). This result has been obtained previously in various forms (Rice 1990; Hartl and Taubes 1998; Welch and Waxman 2003). The derivation based on (Lemma 2 of Cambanis et al. 1981) provides a straightforward alternative (see Supp. Online Text Section 1).

Note that equation (4) assumes that $n > 2$. If $n = 2$, trigonometry on the plane implies that U_i and U_j are fully dependent with $U_j = U_i\rho - \sqrt{1-U_i^2}\sqrt{1-\rho^2}$. If $n = 1$, U_i and $U_j = -1$ or 1 depending on the relative positions of each optima and the reference phenotype. We ignore these particular and simpler cases in most of our derivations.

Moments of the bivariate DFE

We could not obtain a simple bivariate pdf of the fitness effects of mutations across environments in the exact model. However, its cumulant generating function (cgf) has a simple form. It fully characterizes the distribution and provides all its moments. In Supp. Online Text Section 1, we show that the cgf $C_{S_i,S_j}(.,.)$ of the bivariate distribution of fitness effects (S_i, S_j) among random mutations is

$$\begin{aligned} C_{S_i,S_j}\left(t_i, t_j\right) &= \frac{b\lambda}{(1+a\lambda)} - \frac{n}{2}\ln(1+a\lambda) \\ a = t_i + t_j \text{ and } b &= \bar{s}(t_i^2\varepsilon_i + 2\rho t_i t_j\sqrt{\varepsilon_i\varepsilon_j} + t_j^2\varepsilon_j). \end{aligned} \tag{5}$$

It can be checked that this bivariate cgf retrieves the correct distribution for each marginal S_i or S_j, whose stochastic representation is given in equation (3). Indeed, from equation (5), cumulants of any order in S_i and S_j can be obtained as derivatives of $C_{S_i,S_j}(.,.)$ with respect to t_i and t_j, taken at $t_i = t_j = 0$. In particular, it can be checked that the three first central moments / cumulants are consistent with the results in (Martin and Lenormand 2006b). This CGF also provides the fitness correlation across environments:

$$\rho_{ij} = cor\left(S_i, S_j\right) = \frac{1 + 2\rho\sqrt{\varepsilon_i}\sqrt{\varepsilon_j}}{\sqrt{(1+2\varepsilon_i)\left(1+2\varepsilon_j\right)}}. \tag{6}$$

Interestingly, this correlation only depends on the scaled distance to each optima $(\varepsilon_i, \varepsilon_j)$ and the angle between optimal directions (ρ). It measures whether there is a negative mutational trade-off between environments; namely how a mutation that increases or decreases fitness in one environment, results in increased or decreased fitness in the other.

To obtain an intuitive understanding of this equation, we can consider several extreme scenarios. A trivial situation is when the distance to both optima is small ($\varepsilon_i, \varepsilon_j \to 0$). In this case, the angle ψ_{ij} between optimal directions becomes irrelevant to the fitness correlation among random mutants. Most mutations are deleterious and highly positively correlated ($S_i \approx S_j \approx S_d$, $\rho \approx 1$): in the limit, the two environments are confounded. When the reference phenotype is close to at least one of the optima ($\varepsilon_i \to 0$), the correlation decreases with the distance to the other optimum :

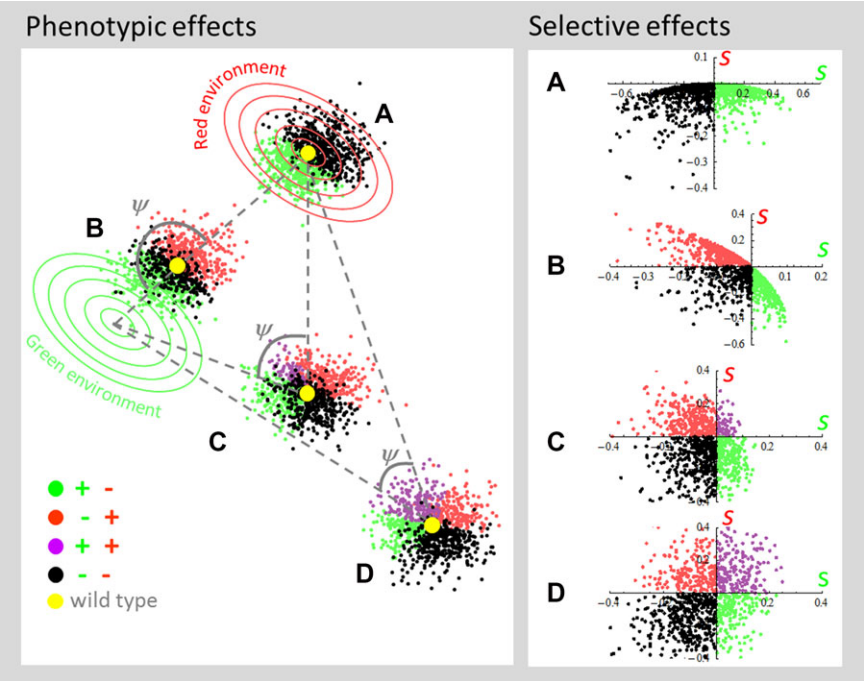

Figure 2. Geometric sketch of fitness trade-offs between environments. Left panel shows the phenotype of random mutations (small dots) around wild types (large yellow dots) in different positions relative to the phenotypic optima of two environments (their corresponding fitness function are represented by red and green contours). Mutations beneficial in the green environment and deleterious in the red (+|–) are represented by green dots, while (–|+), (+|+), and (–|–) mutants are represented in red, purple, and black, respectively. Note that phenotypic positions are projected in only two dimensions, in the plane defined by the position of the wild-type and the two optima. Some mutations appear as (–|–) even though they seem to point toward an optimum. In fact, their phenotypic effect in other dimensions is deleterious, which is not visible on the projection illustrated on the figure. Right panel shows the corresponding bivariate distribution of fitness effect of those mutations. When the wild-type is well adapted to one of the environments (case a), there are very little correlations of mutational effects across environments (ρ) and screening has little effect on the DFE (+|? mutants have a similar DFE in the red environment than ?|? mutants). Strongly screened mutants (++|?) may however exhibit a small "incompressible" cost. In other cases, the angle ψ will determine whether there is a positive or negative ρ. When the wild type is between the two optima (case b), this angle is large ($\cos\psi < 0$) and mutations tend to exhibit antagonistic effects. Here, screened mutants (green dots, +|?) will tend to have large deleterious effects in the no-screen red environment. When the angle ψ is closer to π / 2, (case c, $\cos\psi$ close to 0), ρ is small, with little effect of screening. When the wild type is far from both optima (case d), this angle is small ($\cos\psi > 0$) and mutations will exhibit positively correlated effects between environments (and there is a positive effect of screening).

$\rho_{ij} \approx \left(1 + 2\varepsilon_j\right)^{-1/2}$. Here again, the angle ψ_{ij} has no effect. The angle ψ_{ij} only matters when the reference phenotype is far from both optima ($\varepsilon_i, \varepsilon_j \gg 1$), via $\rho = \cos(\psi_{ij})$. In the limit, this angle entirely determines the correlation: $\rho_{ij} \approx \rho$ when $\varepsilon_i, \varepsilon_j \to \infty$. A geometrical illustration of the effect ρ is given in Figure 2. When the angle ψ_{ij} is wide ($\rho = \cos\left(\psi_{ij}\right) < 0$), there is a negative "trade-off" between environments: a mutant cannot point toward one optimum without pointing away from the other. Conversely, when the angle is narrow ($\rho = \cos\left(\psi_{ij}\right) > 0$), the fitness correlation is positive (positive "trade-off") because a mutant that points toward one optimum also points toward the other. The dependence of ρ_{ij} on ρ and ε_j is illustrated in Figure 3 (also showing the agreement between eq. (6) and exact simulations of the DFE). It is noteworthy that ρ_{ij} never depends on the dimensionality n.

Extension to more than two environments

A natural extension of the model would account for more than two environments. This is challenging in the exact model, but becomes straightforward using a classic approximation to angle distributions in the FGM. As n gets large, the distribution of $U_i = cos(\theta_i)$ in equation (4) converges to a Gaussian with zero mean and variance $1/n$ (matching the exact variance). This property has been used extensively in the context of the FGM to derive approximate distributions in large dimensions (e.g., Hartl and Taubes 1998; Orr 2000; Poon and Otto 2000; Welch and Waxman 2003). Similarly, it can be shown (Supp. Online Text Section 1) that with large n, the pdf of (U_i, U_j) in equation (4) converges to a bivariate Gaussian. This approximation has the advantage to provide a simpler analytic form, especially by

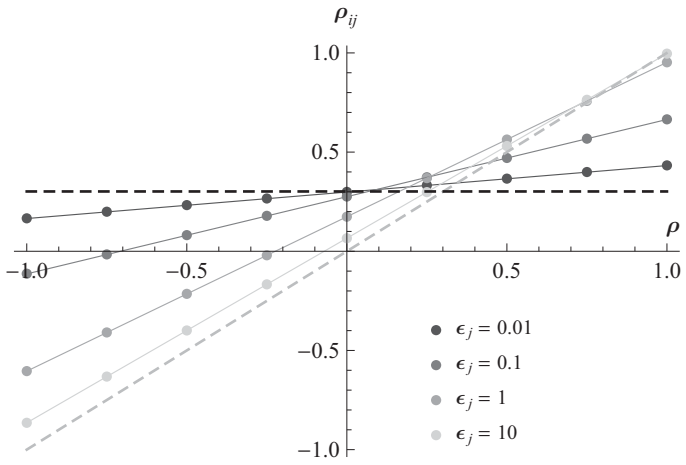

Figure 3. Fitness correlation among environments. The dots show $\rho_{ij} = cor(S_i, S_j)$ versus $\rho = \cos(\psi_{ij})$, across two environments i and j, for varying distances from the wild type to the optimum in environment j (ε_j in legend). The distance to the optimum in environment i was fixed to $\varepsilon_i = 5$. The dots show exact simulations and the plain lines show the corresponding (exact) prediction from equation (6), the horizontal thick black dashed line shows $\rho_{ij} = 1/\sqrt{1+2\varepsilon_i}$ (limit when $\varepsilon_j \to 0$) and the thick gray dashed line shows $\rho_{ij} = \rho$ (limit when $\varepsilon_j \to \infty$). Other parameters and simulation methods as in Figure 1, except that the vector $\mathbf{z}_j$ was set as $\mathbf{z}_j = \sqrt{2\varepsilon_j}\mathbf{s}\mathbf{u}_1$, then rotated (on the two first dimensions) to obtain a given $\rho = \mathbf{z}_i.\mathbf{z}_j/\mathbf{z}_i.\mathbf{z}_j$.

avoiding the truncation ($0 < u_i^2 + u_j^2 - 2\rho u_i u_j < 1 - \rho^2$) inherent to equation (4). It can also easily be extended to an arbitrary number K of environments, where the stochastic representation in equation (2) is best expressed in vector form. More precisely, let $\mathbf{U} = \{U_i\}_{i\in[1,K]}$ be the vector of angle cosine in each of the K environments: the Gaussian approximation states that $\lim_{n\to\infty} \mathbf{U} = \mathbf{U}^G$ where $\mathbf{U}^G = \left\{U_i^G\right\}_{i\in[1,K]}$ follows a multivariate Gaussian (hence the "G") with mean zero, variance $1/n$ and appropriate pairwise correlations $\cos\psi_{ij} = \mathbf{z}_i.\mathbf{z}_j/(z_i z_j)$ for each pair of environments (i, j). The corresponding large n approximation for the vector $\mathbf{S} = \{S_i\}_{i\in[1,K]}$ of DFEs in each of the K environments is $\mathbf{S} \approx R\zeta.\mathbf{U}^G - R^2 1_K/2$ where $R^2 \sim \Gamma(n/2, 2\lambda)$ is the magnitude of mutation effects (common to all environments), $1_K = \{1, .., 1\}$ and $\zeta = \{z_i\}_{i\in[1,K]}$ contains all phenotypic distances to each optimum. As for the two-environment version, this approximation yields the exact multivariate moments up to order three; discrepancies arise at higher order. This approximation has the advantage of easily generalizing to n environments. However, it has two potential limitations. First, it does not accurately capture the tail of the distribution of $\mathbf{U}$, even for large n. This could be problematic when describing the subset of the few fittest beneficial mutants. Second, the dimensionality n may not always be large enough for the approximation to hold, even for the bulk of mutations (roughly, it breaks down below $n = O(5)$).

DISTRIBUTION OF CONDITIONAL FITNESS EFFECTS $S_j|S_i$

The above derivations yield the DFE among random (?|?) mutants. However many applications of the model must deal with the effect S_j, in environment j, of a subset of mutants conditioning on their effect in environment i (on their s_i), for example conditional on $S_i > 0$ ((+|?) mutants). We denote "selective environment" the environment i where a selection "filter" is applied; namely where mutants may be screened or selected. We denote the conditional variable $S_j|S_i = s$ the random variable S_j among the set of mutants with selective effect S_i lying within the infinitesimal domain $S_i \in [s, s + ds]$. We call the distribution of $S_j|S_i = s$ the "conditional DFE."

Conditional DFE in the general case

The conditional DFE can be derived or simulated directly from the stochastic representation of each variable ($S_i = RU_i z_i - R^2/2$, $S_j = RU_j z_j - R^2/2$) and equation (4), but it does not take a simple general form. A detailed description can be found in Supp. Online Text Section 2. A simpler but only approximate expression can be found when considering a wild type that is not well adapted to the selective environment i (when $\varepsilon_i \gg 1$). This situation is often the most relevant case biologically (when substantial adaptation takes place in i), and it allows several key simplifications (see Supp. Online Text Section 2). In this limit, most mutations have mild effects in the selective environment, relative to the distance to the optimum: the scaled selective effect S_i/s_o^i is small for most mutations. Together, $\varepsilon_i \gg 1$ and $S_i \ll s_o^i$ allow key simplifications regarding the conditional DFE. The conditional effect $S_j|S_i$ can be written as a nonlinear regression on the selective effect S_i, namely as the sum of a deterministic function of S_i ($\omega(S_i)$) plus a random 'error' term ξ which is distributed independently of s. Define the two constants $\xi_o = s_o^j(1-\rho^2)/(1-\rho\nu)$

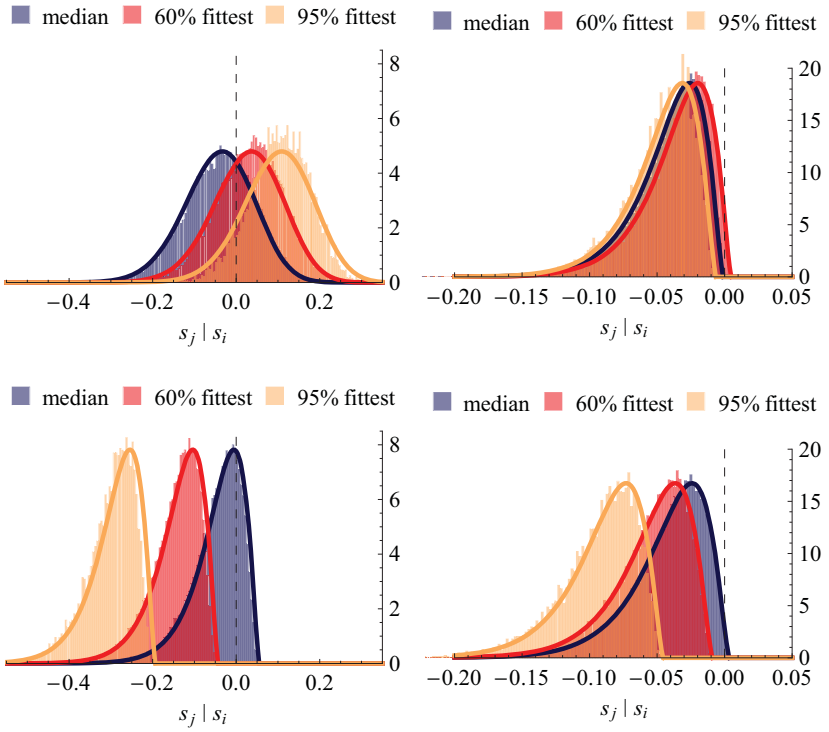

Figure 4. Conditional distribution of $s_j|s_i$. Histograms show the conditional distribution of $S_i|S_j$. We simulated S_i for 10^6 random mutants with $\varepsilon_i = 10$. Then, for a given fixed value of s, we sampled the subset of mutants with effect S_i lying within $S_i \in [s, s + ds]$ with width $ds = 0.03s_o^i$. The observed distribution is compared to the theory (plain lines) for $S_i|S_j$ derived from equation (7). Each panel presents results for three quantiles of s: the median of the distribution of S_i (bulk of the DFE in environment i), the top 10% fittest and the top 0.5% fittest (extreme right tail of the DFE). The top panels correspond to $\rho = 0.7$ and the bottom panels to $\rho = -0.95$, while the left panels correspond to $\nu = 0.9$ and the right panels to $\nu = 0.1$. Other parameters and simulation methods as in Figures 1 and 3.

and $\lambda_\xi = \lambda(1 - \rho\nu)$ where $\lambda = 2\bar{s}/n$ is the scaling constant and $\nu = \sqrt{\varepsilon_j/\varepsilon_i}$ describes the maladaptation to environment j relative to i. We get the following stochastic representation:

$$\begin{aligned} S_j|S_i &\approx \omega(S_i) + \xi \\ \omega(s) &= \rho\nu s - (1 - \rho\nu)\, s_o^i \gamma^*_{min}(s) \\ \xi &= \xi_o - \tfrac{\lambda_\xi}{2}\chi^2_{n-1}\left(2\xi_o/\lambda_\xi\right) \end{aligned}, \qquad (7)$$

where $\gamma^*_{min}(s) = 2 - s/s_o^i - 2\sqrt{1 - s/s_o^i} \approx (s/s_o^i)^2/4$. Note that the approximation can only be valid if $\xi_o > 0$, namely if $\nu < 1/\rho$ whenever $0 < \rho < 1$ (there is no constraint when $\rho < 0$). This condition is always met when $\nu < 1$, namely when the wild type is better adapted to environment j than i. The conditional pdf of $S_j|S_i$ is easily obtained from this stochastic representation, as ξ has the same representation (with modified parameters) as S_i, whose pdf is given in equation (3). The pdf of ξ is $f_\xi(\xi) = f_S\left(\xi, n - 1, \lambda_\xi, \xi_o\right)$, and the pdf of $S_j|S_i$ conditional on $S_i = s_i$ is thus given by

$$f_{S_j|S_i}\left(s_j, s_i\right) \underset{\varepsilon_i \gg 1}{\approx} f_S\left(s_j - \omega(s_i), n - 1, \lambda_\xi, \xi_o\right) \qquad (8)$$

This conditional distribution is a central result: it yields the distribution of the correlated fitness effects S_j of any class of mutants (defined from some criterion on its selective effects $S_i = s_i$).

The distribution of $S_j|S_i$ is illustrated in Figure 4, for three classes of mutant selective effects s_i (median effect, 60% fittest, 95% fittest). Equation (7) is accurate for various values of ρ and ν with a wild type lying at substantial distance from the selective optimum ($\varepsilon_i = 10$). The accuracy is slightly lessened for very fit mutants (yellow histograms, 95% fittest) namely outside the bulk of the distribution of S_i. The effect of ρ via $\rho\nu s_i$ is most visible by the shift of the distribution for the fittest mutant class (compare right vs. left panels). The approximation in equation (7) seems robust: it is still accurate under mild maladaptation to environment i (Fig. S3A, at $\varepsilon_i = 2$); it breaks down closer to the optimum (Fig. S3B, at $\varepsilon_i = 0.5$), although, even then, $S_j|S_i$ is still well predicted among median genotypes.

Situations where conditioning has no impact

Equation (7) identifies cases where screening in environment i has little impact on fitnesses in environment j. A first case is

when the two optima point towards roughly orthogonal directions ($\rho = \cos\psi \ll 1$). The fitness correlation between environments typically becomes negligible (eq. (6) and equation (7) simplifies : $\xi_o = s_o^j\left(1-\rho^2\right) \approx s_o^j$, $\lambda_\xi = \lambda(1-\rho\nu) \approx \lambda$ and the dependence to s ($\omega(s) \approx -s_o^i\gamma^*_{min}(s) \approx -\left(s/s_o^i\right)^2/4$) becomes negligible for the bulk of mutations ($s \ll s_o^i$). The distribution of $S_j|S_i$ converges to that of $\xi \approx s_o^j - \lambda/2\chi^2_{n-1}(2s_o^j/\lambda)$, which itself converges to that among random mutants: $S_j = s_o^j - \lambda/2\chi^2_n(2s_o^j/\lambda)$ (eq. (3), where $\chi^2_n \approx \chi^2_{n-1}$ whenever $n \approx n-1$. Therefore when optimal directions are orthogonal, conditioning on a given effect in environment i has negligible effect on the resulting DFE in environment j: the observed DFE is similar to that among random mutations.

A second case is when the wild type is much better adapted to environment j than i ($\nu \to 0$). Again for the bulk of mutations, $S_j|S_i \sim \xi_o - \lambda/2\chi^2_{n-1}(2\xi_o/\lambda)$ is independent of s. This is illustrated on the top right panel of Figure 4 ($\nu = 0.1 \ll 1$), where the conditional DFEs are very similar for widely differing mutant classes (while optimal directions are not orthogonal $\rho \neq 0$). Furthermore, as $\xi_o = s_o^j(1-\rho^2)$, this DFE converges to that of random mutants whenever $\rho^2 \ll 1$ so that $\xi_o \approx s_o^j$ (see orthogonal case) or $s_o^j \to 0$ so that $\xi_o \approx 0$, still provided $n \approx n-1$.

"Cost" distribution

An interesting subcase is when the wild type is well adapted to environment j ($s_o^j \to 0$). This situation is frequently investigated when considering the "costs of adaptation," that is the effect in environment j of mutants that are beneficial in i (e.g., cost of antibiotic resistance genes). As seen above, this cost is then independent of S_i for the bulk of mutations. This cost distribution is then a negative gamma : $S_j|S_i \sim -\Gamma((n-1)/2, \lambda)$, similar to that of random mutants ($S_j \sim -\Gamma(n/2, \lambda)$).

A more precise treatment is possible: setting $s_o^j \to 0$ (and thus $\varepsilon_j \to 0$ and $\nu \to 0$) in equation (7), implies substantial simplifications. The conditional DFE then becomes

$$S_j|S_i \underset{\substack{\varepsilon_j \to 0 \\ \varepsilon_i \gg 1}}{\approx} -s_o^i\gamma^*_{min}(S_i) - \Gamma\left(\frac{n-1}{2}, \lambda\right). \quad (9)$$

The conditional DFE consists only of deleterious ("costly") effects and entails an "incompressible cost" : $S_j|S_i \leq -s_o^i\gamma^*_{min}(S_i) \approx -S_i^2/(4s_o^i)$. This reflects the fact that any mutation (beneficial or not in i) must move the phenotype away from the wild type's position (which is optimal in j), reducing fitness in j.

Bivariate pdf of S_i, S_j

Finally, a straightforward application of equations (7) and (8) is to derive an approximate bivariate pdf for the joint distribution of fitness effects (S_i, S_j) in both environments, among random mutants (?|?). This can be used to fit empirical datasets, in order to test the model's predictions and/or estimate its parameters in particular species/environments. It can also be plugged into theoretical models of evolution in heterogeneous environments. By basic properties of conditional probability density functions, this joint pdf is simply $f_{S_i,S_j}\left(s_i, s_j\right) = f_S\left(s_i\right) f_{S_j|S_i}(s_i, s_j)$, namely

$$f_{S_i,S_j}\left(s_i, s_j\right) \approx f_S\left(s_i, n, \lambda, s_o^i\right) f_S(s_j - \omega\left(s_i\right), n-1, \lambda_\xi, \xi_o), \quad (10)$$

where the pdf $f_s(.)$ is given in equation (3), while the function $\omega(.)$ and the coefficients λ_ξ and ξ_o were introduced in equation (7). This pdf will be illustrated below.

COMPARISON TO ANISOTROPIC SIMULATIONS

Our theoretical results assume isotropy, where all directions in phenotype space are equivalent (for selection and mutation), so that polar coordinates are statistically independent. However, anisotropy of mutational and selective effects may have an important influence on mutational effects (Martin and Lenormand 2006b). It can be introduced by mutational or selective correlations, and/or heterogeneity in mutational variance or strength of stabilizing selection across traits (Lande 1980). These effects may in addition differ between environments, for example if different combinations of traits are favored in different environments ("syndromes") or if mutational variances and covariances change with the environment ("phenotypic plasticity").

The central effect of anisotropy is that directions in phenotypic space matter, not only distances. We showed previously (Martin and Lenormand 2006b) that in single environments, mild anisotropy could be absorbed into an isotropic model with a reduced "effective" dimensionality. In supplementary text, we study when such modified isotropic model corrects for anisotropy in multiple environments, and explore this effect by simulation (Supp. Online Text Section 3, Fig. 5 and Fig. S4).

Figure 5 shows the bivariate pdf of (S_i, S_j) in mildly anisotropic simulations versus the isotropic theory in equation (10). In this example, anisotropy is mild but not negligible (selection strength varies by a factor $1.5-2$ across traits), and is environment dependent (covariances change across environments). The different panels illustrate how the distribution changes with ρ and ν. The agreement between simulations and theory is generally good. Note that the bottom panels ($\nu = 0.05$) illustrate how the effect of ρ becomes less important when the wild type is much more adapted to environment j than i: the distributions are fairly similar although ρ is very different across panels ($\rho = -0.9$ or 0.7). Conversely, the angle between optimal directions (via ρ) drives the covariance pattern in the top panels, where maladaptation is substantial in both environments ($\nu = 0.3$). Figure S4 illustrates how discrepancies arise with equation (10) as anisotropy becomes stronger. Part of these discrepancies can be corrected for within

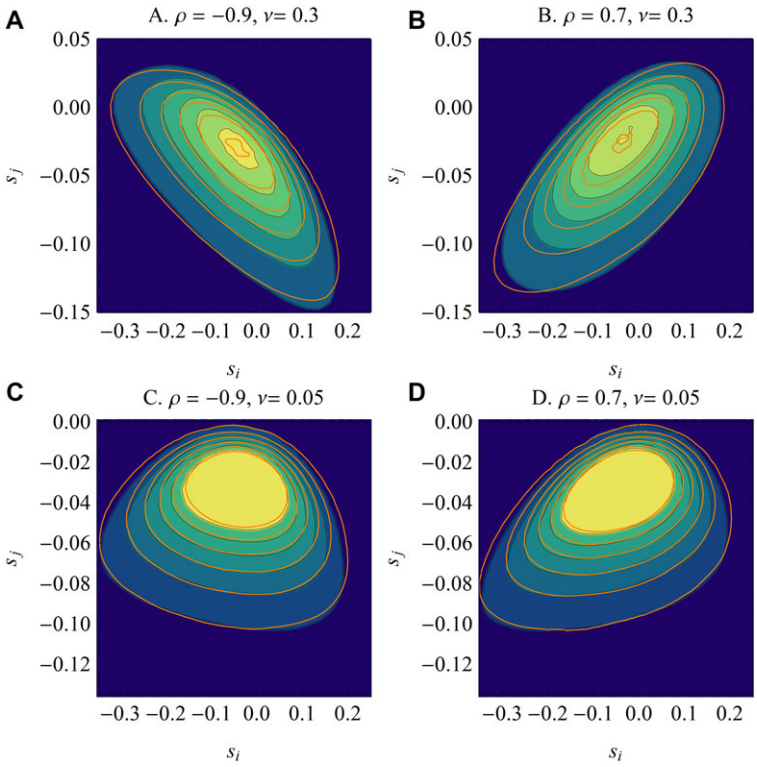

Figure 5. Bivariate distribution of (S_i, S_j) with mild anisotropy. The bivariate probability density of (S_i, S_j) among random mutants (blue-green contour plot) is compared to the prediction from equation (10) (orange lines). The parameters and simulation methods are the same as in Figures 3 and 4, except for anisotropy: this time, the mutant phenotypes ($dz \sim N(0, \lambda I_n)$ as previously) have fitness effect $S_i = dz.S_i.z_i - dz.S_i.dz/2$, where S_i is the matrix of selective covariance in environment i, and the same goes for S_j in environment j. Matrices S_i and S_j were drawn independently (environment-dependent anisotropy), as Wishart deviates: $S \sim W_p(I_n)$ with $p > n$ determining the level of anisotropy. They were then scaled so that $\bar{s} = n\lambda/2$. Here $p = 30n$ so that anisotropy remains relatively mild. Panels A–D correspond to distinct values of ρ and ν indicated on the graph.

the model (Supp. Online Text Section 3) but not when anisotropy is strong.

APPLICATION: ADAPTATION IN A METAPOPULATION WITH TWO HABITATS

The single-peak FGM has been used to extend single-allele population genetics to genome-wide context-dependent processes (Orr 1998; Orr 2000). We can now transpose this approach to a multiple-peak FGM. This may encompass spatial or temporal variation, sex or stage-dependent fitness functions etc., provided that distinct contexts determine distinct optima and that isotropy remain a good enough approximation. Here, we detail one possible application (among many other possibilities) where this model is used to develop a genome-wide theory of adaptation (with variable mutational effects), across multiple contexts. We consider adaptation in a metapopulation (island model with strong symmetric migration at rate m) divided into two habitats (i and j in relative proportion ϕ and $1-\phi$ among demes) characterized by distinct optima. Mutations arise over the whole genome of a given background, which phenotypic position, relative to each optimum, determines (ε_i, ε_j, ρ) and thus the joint DFE of (S_i, S_j) following our model. We study the probability that such one-step mutation (assuming codominant alleles or haploids) gets fixed or lost in the whole metapopulation. In variable environments, fixation probabilities depend on the relative strengths of migration, drift, and selection and no general purpose expressions are known (reviewed in Whitlock and Gomulkiewicz 2005). However, the problem simplifies in the "strong migration limit" ($m \gg \bar{s}, 1/N_e$) where the fixation probability of a single-copy mutant is approximately (Nagylaki 1980; Whitlock and Gomulkiewicz 2005) : $\pi_f(\tilde{S}) \approx (1-e^{-\alpha\tilde{S}})/(1-e^{-2\alpha N_e\tilde{S}})$, where $\tilde{S} = S_i\phi + S_j(1-\phi)$ is the mean S over the metapopulation, α is a coefficient and N_e is the effective size, both depending on demographic details (assumed constant across habitats). Typically, the coefficient is $\alpha = 2$ but it may be modified by ploidy, extinction/recolonization dynamics, population structure etc. (Barton and Whitlock 1997). Let U be the genomic mutation rate, the rate of substitution is $k = UE(\pi_f(\tilde{S}))$, and the rate of adaptation (change in mean log-fitness) is $\partial_t \overline{\log W} = UE(\tilde{S}\pi_f(\tilde{S}))$.

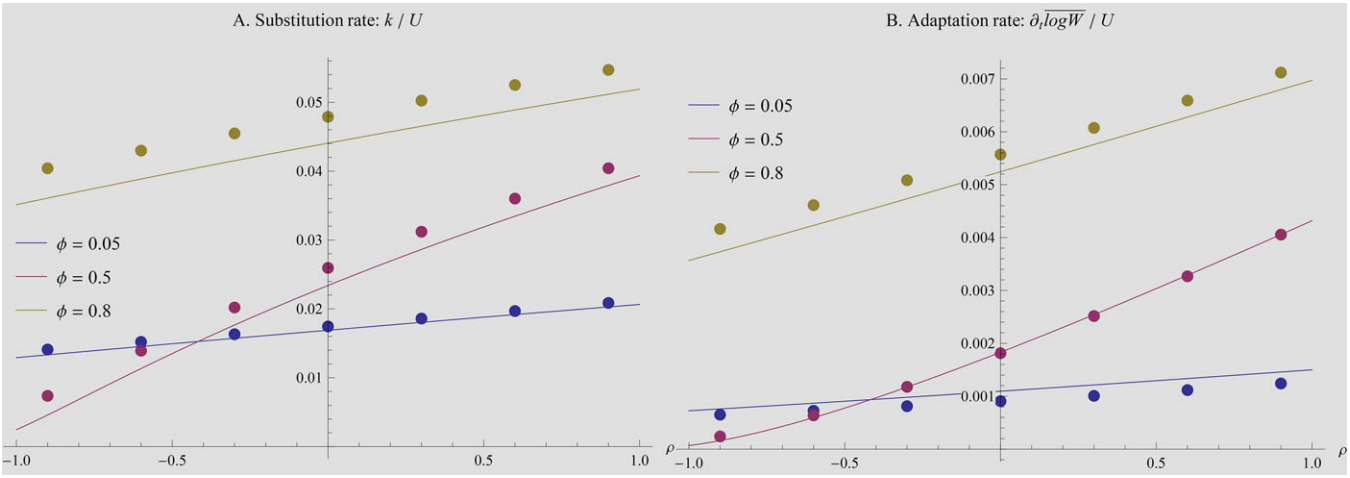

Figure 6. Rate of adaptation in heterogeneous conditions. The rate of (A) substitution and (B) adaptation were computed from exact simulations of the distribution of (S_i, S_j) (same as Fig. 5), according to the formulae for a high migration regime: $k = UE(\pi_f(\tilde{S}))$ and $\partial_t \overline{\log W} = UE(\tilde{S}\pi_f(\tilde{S}))$ using the exact diffusion formula for fixation proabilities $\pi_f(.)$ (see text). The dots show the results (scaled by the mutation rate U) from these simulations for various levels of mutational correlation (ρ, x-axis) and proportions of habitat i (ϕ indicated in legend). The lines show the corresponding predictions from equation (11). The fitness distances to each optimum were $\varepsilon_i = 12$ and $\varepsilon_j = 3$.

From equation (5), it is easily shown (Supp. Online Text Section 4) that any linear combination of S_i and S_j is distributed exactly as the DFE in a single environment (given in eq. (3)), with modified coefficients λ and s_o. In the particular case of habitat heterogeneity and strong migration, the relevant variable $\tilde{S}$ is distributed as in equation (3), with modified fitness distance to the optimum: $\tilde{s}_o = s_o^i\left(\nu^2 + \xi^2 + 2\nu\xi\rho\right)/(1+\xi)^2$ where $\nu = \sqrt{\varepsilon_j/\varepsilon_i}$, as previously, and $\xi = \phi/(1-\phi)$. Note however, that this result is a weak selection limit: the approximation for $\pi_f\left(\tilde{S}\right)$ arises in a discrete time model while our model (eq. (1)) yields an average of the continuous time equivalent selection coefficients. The approximation is valid whenever $e^s - 1 \approx s$. This de facto transforms the possibly multi-peaked fitness surface in discrete time (mixture of two Gaussian functions) into a single-peaked effective fitness surface in continuous time coefficients (log of the geometric mean of two Gaussian functions) through the log-scaling. This explains why we retrieve a simple representation for $\tilde{S}$ in terms of an effective single-peak DFE.

Furthermore, this single-environment DFE becomes approximately normal when the wild type is sufficiently maladapted that $\tilde{s}_o \gg \bar{s}$ (Supp. Online Text Section 3): the distribution of $\tilde{S}$ then converges to a Gaussian with mean $-\bar{s}$ and standard deviation $\sigma = 2\bar{s}\sqrt{\tilde{s}_o/n}$. Assuming $N_e\bar{s} \gg 1$, the rates of substitution and adaptation, at the metapopulation scale, are thus respectively

$$k \approx \frac{U}{2}\left(Erfc\left(\frac{\bar{s}}{\sqrt{2}\sigma}\right) - e^{\frac{\alpha^2\sigma^2}{2}+\alpha\bar{s}}Erfc\left(\frac{\alpha\sigma^2+\bar{s}}{\sqrt{2}\sigma}\right)\right)$$

$$\partial_t\overline{\log W} \approx \frac{U}{2}\left(e^{\frac{\alpha^2\sigma^2}{2}+\alpha\bar{s}}Erfc\left(\frac{\alpha\sigma^2+\bar{s}}{\sqrt{2}\sigma}\right)\left(\alpha\sigma^2+\bar{s}\right) - Erfc\left(\frac{\bar{s}}{\sqrt{2}\sigma}\right)\bar{s}\right) \quad (11)$$

Where $Erfc(.)$ is the complementary error function. The dependence of these rates on the geometry of the landscape (ρ) and the proportion of each habitat (ϕ) is illustrated on Figure 6. In the simulations with small effective size ($N_e = 200$), the expectations are computed with the fixation probability $\pi_f(\tilde{S})$, from the diffusion approximation, allowing for the fixation of deleterious mutations, while they are neglected in equation (11). The prediction for k in equation (11) is robust to fairly small $\varepsilon_i, \varepsilon_j$ while that for $\partial_t\overline{\log W}$ tends to overestimates the actual rate in this case (compare Fig. 6 A vs. B), unless $\varepsilon_i + \varepsilon_j > 10$. As expected, the prediction is more accurate under weaker selection ($\bar{s} = 10\%$vs.1%in Fig. S5).

Discussion

DISTRIBUTION OF FITNESS EFFECTS OF MUTATIONS ACROSS ENVIRONMENTS

We consider an extension of Fisher's geometric model (FGM), where different environments determine distinct phenotypic optima. The joint distribution of fitness effects (DFE) of mutation in different environments (distribution of (S_i, S_j) for environments i and j) depends, as expected, on the same basic parameters that determine the DFE in each environment (Fig. 2): the number of dimensions n, the scale λ, and the distance to each optimum $(\varepsilon_i, \varepsilon_j)$. These few parameters all have a clear biological interpretation (Martin and Lenormand 2006a). However, an extra parameter influences the multivariate DFE: the angle ψ between the wild-type phenotype and the direction to each optimum (illustrated on Fig. 2 and eq. (10). The cosine of this angle ($\rho = \cos\psi$) partly

determines the fitness correlation across environments. When the wild type is maladapted to both environments, this correlation is approximately equal to ρ. On the contrary, when the wild type is well adapted to one of the two environments, the fitness correlation is always positive and decreases with increased maladaptation to the other environment. Beyond these theoretical insights, equation (10) provides a density function that can be fitted to multivariate empirical fitness data across environments, extracting all the information from this data. These could be applied (together with the relevant statistical framework) to the wide set of empirical studies of DFEs across environments, including both single mutations and mutation accumulation lines (see Introduction). In particular, the angle ψ between the wild type and optimal phenotypes can be inferred from an estimate of the parameter ρ in equation (10). In principle, this could be used to empirically determine whether different environments determine optima that lie on the same line, same plane etc.

SCREENED VERSUS RANDOM MUTANTS

Our results also clarify the expected effects of screening on DFEs. Several experimental studies have used screening as an efficient way to retrieve mutants (see Introduction). The data were interpreted assuming that the resulting DFE in some (no-screen) environment was representative of the effects of random mutations. The conditional DFE in equation (7) and Figure 4 clarifies when this can be expected or not.

First, the DFE in the no-screen environment indeed converges to that among random mutations (in the same environment) when (i) the wild type is much better adapted to the no-screen than to the screen environment ($\nu \to 0$, eq. (7) or when (ii) the two optima point toward orthogonal directions ($\rho = \cos\psi = 0$). Case (i) may provide an efficient method to obtain the DFE among random mutants, given that screening is faster and cheaper than the random mutagenesis typically used for this purpose. Cases (i) and/or (ii) are qualitatively consistent with the results of Trindade et al. (2012). First, they found, in several no-screen environments, that the DFE estimated from screened mutants had the form expected for random mutants in Fisher's model (displaced gamma similar to eq. (1). Second, they showed that this DFE correctly predicted the outcome of experimental adaptation (from random de novo mutations) in each of the no-screen environments. This might be surprising at first given that the mutant used for prediction were not random (they were screened). In fact, as explained above, screened and random mutants may share similar distribution under specific conditions. In particular, as we showed, this outcome is expected when the wild type is much less adapted to the screening environment than the no-screen environment ($\nu \to 0$). This is probably the case in this study: in the three no-screen environments, the fitness distance of the wild type to the optimum ($\xi_0 = s_0^j$, inferred from the displaced gamma fit) was small relative to the corresponding distance (s_0^i) expected in the screening environment (antibiotic).

Second, in all other cases, screened mutants have a different DFE compared to random mutants in the no-screen environment. In particular, the DFE of screened mutants can exhibit positive skewness, which is never expected for random mutants. This can only occur when the wild type is maladapted to both environments and the angle ψ is narrow, which should also cause positive fitness correlation between screen and no-screen environments ($\rho \to 1$). This situation matches the observation in (Kassen and Bataillon 2006), where the fitness correlation between screen and no-screen environments was strongly positive (suggesting $\rho \to 0$ and $\nu \neq 0$) and where the DFE of screened mutants in no-screen conditions was positively skewed.

Finally, note that the set of mutants studied can also be those sequentially fixed during a bout of adaptation. This differs from a set of replicate single-step fixations and would require a full treatment of its own.

SELECTIVE AND MUTATIONAL TRADE-OFF ACROSS ENVIRONMENTS

During adaptation to a single environment, FGM predicts that the distribution of fitness effects shifts towards more and more deleterious effects (Orr 2000). Similarly here, adaptation to a pair of environments connected by migration (say, a pesticide-treated and untreated area) will result in bivariate distribution of effects that will shift progressively towards negative correlations (e.g., a typical trajectory would go from cases d to c, and then b on Fig. 2). Applying the present model to this situation should allow to capture the dynamics of genetic trade-offs emerging from the interplay of mutation and adaptation in heterogeneous conditions, instead of considering it fixed from the start, as is typical in existing models. Such trade-off dynamics was also empirically demonstrated in (Jasmin and Zeyl 2013). The model makes explicit the distinction between two forces determining the pattern of covariance in fitness across environments: (i) the mutational covariance in fitness, which changes as the relative position of the wild type and the two optima evolves, and the selective trade-off, which is fixed and set by the distance between the optima, scaled by the width of the fitness functions. The former should drive the transient pattern of fitness correlation, while the latter is mostly affecting the ultimate pattern of local adaptation and specialization (or lack thereof), as described in Levins's (1968) concept of "fitness sets." This tension between processes impacting the covariance among fitness components shares many similarities with allocation-acquisition models, used in life history theory (Roff and Fairbairn 2007).

EXTENDING THEORIES OF ADAPTATION

Beyond direct tests based on empirical studies of the DFE, the mutational model proposed here can also be plugged into adaptation

theories (incorporating selection, drift, and migration). This may help handle context-dependence at a genome wide scale, with a variety of potential applications.

The first direct application is to study adaptation to heterogeneous environments. As an illustration of how such theory can be developed, we computed (eq. (11)) the expected rates of substitution and of adaptation (averaged over the genome, hence over the DFE) in a metapopulation undergoing mutation, drift, migration, and heterogeneous selection. We considered two habitats in some arbitrary proportion, high migration relative to selection and a wild type initially maladapted to both environments. Both rates are highly dependent on the geometry of the landscape (Fig. 6). When the angle toward the new optimum is small (large $\rho > 0$ on Fig. 6), the rates of adaptation and substitution increase when the most challenging habitat (whose optimum is the farthest) is more prevalent (higher ϕ on Fig. 6). On the contrary, when the angle toward the new optimum is wide (large $\rho < 0$ on the Fig. 6), adaptation and substitutions are slowest when the two habitats tend to be in equal proportion such that the selective antagonism is maximized ($\phi = 0.5$ on Fig. 6). This is intended as an illustration: a full treatment would have to include the pattern of polymorphism maintained across the genome (local adaptation at lower migration rates, see e.g., Yeaman and Otto 2011), and the iteration of adaptive steps (full trajectory). Such treatment will likely be more challenging (especially keeping track of the angle ψ over time), but would also rely on the mutational model proposed here.

Again, these results apply to any context where adaptation stems from a linear combination of fitnesses in multiple contexts (each determining a distinct optimum), potentially including sexes (Connallon and Clark 2014), life history traits (survival/reproduction, e.g., eq. (3) of Ronce and Olivieri 1997), stages (Barfield et al. 2011), or age-classes (Moorad and Hall 2009,Cotto 2014 #3093). This would be an interesting application as much of life history theory relies on well capturing phenotypic correlations and constraints arising from mutational covariances and selective trade-offs (Roff and Fairbairn 2007). A second application would be to predict the mean correlated fitness change, in any environment j, due to adaptation in some fixed selective environment i. The conditional distributions of $S_j|S_i$ (eqs. (7)–(9) can be used to predict these average "costs of specialization," for example along an ecological gradient, provided that this gradient can be simply mapped to a series of phenotypic optima. As could be qualitatively anticipated, adaptation to new conditions, from optimal conditions (eq. (9)) entails an "incompressible cost" reflecting the fact that screened mutants (++|?) are necessarily (++|–) mutations, due to the incompressible selective trade-off among phenotypic optima across environments. Yet, quantitative analysis shows that this effect is surprisingly small: very strong screening (e.g., 95% fittest class in Fig. 4) is required to see a clear quantitative impact.

DEVIATIONS FROM THE MODEL'S ASSUMPTIONS

The model relies on four key simplifying assumptions: (i) isotropy (all directions equivalent), (ii) absence of plasticity (environmental shifts do not affect the underlying phenotypes), (iii) common landscape (environments differ only in phenotypic optima), and (iv) universal pleiotropy (all mutations considered affect the same set of traits, no modularity). The model proves robust to mild anisotropy (i), even if it varies across environments (ii) (Fig. 5 and Fig. S4), whenever mutation effects retain a constant scale across environments (constant mean $\bar{s}$). However, fitness effects may also scale differently across conditions ($E(S_i) \neq E(S_j)$), which can be detected in the lab. A previous review and analysis of empirical DFEs across environments (Martin and Lenormand 2006a) suggested that such variation was small relative to changes in the fitness variance across mutants (the latter pattern being consistent with the basic FGM used here). Yet such changes in scale may be accounted for by simply rescaling the model for each environment, that is letting $\lambda \to \lambda_i$ or λ_j in each environment, and scaling the multivariate distribution and its CGF accordingly (eqs. (5)–(10).

Two assumptions remain more limiting. With strong plasticity (ii), phenotypic traits shift across environments in the absence of mutations, which should cause deviations from the model's predictions (at least when the plastic traits contribute largely to fitness). Including these effects would require extending the geometry of the present model: possibly by introducing a genetically determined reaction norm with the environment (see e.g., Gomulkiewicz and Kirkpatrick 1992) or simply by summing a constant genotypic contribution to phenotype and one that randomly varies across environments (thus with tuneable correlation across environments as in Via and Lande 1985). It would also require to relate these parameters to empirically measurable quantities. Similarly, strong modularity (iv), where different sets of traits are affected by different genomic targets would likely create deviations from the model's predictions. For example, different modules may contribute to adaptation in different environments if they yield variation along different directions. Both deviations are worth exploring: the former holds the key to the evolution of adaptive plasticity and the latter to parallel evolution (Chevin et al. 2010). Empirically, the detection of modularity effects requires DFEs, across environments, among mutant sets with distinct, known, genetic targets. Such data have become amenable to measurement with the advent of high-throughput phenotyping methods (e.g., Hietpas et al. 2013). We hope that this model can be used as a null model in this respect: deviations can be detected empirically, by straightforward statistical rejection

methods, and different experiments can be compared within this framework.

ACKNOWLEDGMENTS

We thank two anonymous reviewers and the editors for their help in improving this manuscript, and Thomas Bataillon, Rees Kassen, Craig MacLean and Ophélie Ronce, for stimulating feedback on an earlier version of this manuscript. This work was funded by Agence Nationale de la Recherche (ANR Silentadapt N°100517, ANR EVORANGE ANR-09-PEXT-011), CNRS (PEPII INSB-INEE-INSMI-INS2I) and Agropolis Fondation (Montpellier, France) under the reference ID « BIOFIS » 1001–001". This is ISEM publication N° 2015–075.

DATA ARCHIVING

https://datadryad.org/resource/doi:10.5061/dryad.8dg19.

LITERATURE CITED

Agrawal, A. F., and M. C. Whitlock. 2010. Environmental duress and epistasis: how does stress affect the strength of selection on new mutations? Trends Ecol. Evol. 25:450–458.

Barfield, M., R. D. Holt, and R. Gomulkiewicz. 2011. Evolution in stage-structured populations. Am. Nat. 177:397–409.

Barton, N. H., and M. C. Whitlock. 1997. The evolution of metapopulations. Pp. 183–210 *in* H. I.A., and G. M.E., eds. Metapopulation biology. Academic Press, 32 Jamestown Road, London, NW1 7BY, UK.

Bataillon, T., T. Y. Zhang, and R. Kassen. 2011. Cost of adaptation and fitness effects of beneficial mutations in pseudomonas fluorescens. Genetics 189:939–U317.

Bell, G. 2008. Experimental evolution. Heredity 100:441–442.

Cambanis, S., S. Huang, and G. Simons. 1981. On the theory of elliptically contoured distributions. J. Multivar. Anal. 11:368–385.

Chevin, L. M., G. Martin, and T. Lenormand. 2010. Fisher's model and the genomics of adaptation: restricted pleiotropy, heterogenous mutation, and parallel evolution. Evolution 64:3213–3231.

Connallon, T., and A. G. Clark. 2014. Evolutionary inevitability of sexual antagonism. Proc. R Soc. B Biol. Sci. 3:281.

Consortium, R.E.X. 2010. The skill and style to model the evolution of resistance to pesticides and drugs. Evol. Appl. 3:375–390.

Cotto, O. and O. Ronce. 2014. Maladaptation as a source of senescence in habitats variable in space and time. Evolution 68:2481–2493.

Duputie, A., F. Massol, I. Chuine, M. Kirkpatrick, and O. Ronce. 2012. How do genetic correlations affect species range shifts in a changing environment? Ecol. Lett. 15:251–259.

Fisher, R. A. 1930. The genetical theory of natural selection. Oxford Univ. Press, Oxford.

Fry, J. D. 1993. The "general vigor" problem: can antagonistic pleiotropy be detected when genetic covariance are positive? Evolution 47:327–333.

Fry, J. D. 1996. The evolution of host specialization: are trade-offs overrated? Am. Nat. 148:S84–S107.

Fry, J. D., and S. L. Heinsohn. 2002. Environment dependence of mutational parameters for viability in *Drosophila melanogaster*. Genetics 161:1155–1167.

Gomulkiewicz, R., and M. Kirkpatrick. 1992. Quantitative genetics and the evolution of reaction norms. Evolution 46:390–411.

Gordo, I., and F. Dionisio. 2005. Nonequilibrium model for estimating parameters of deleterious mutations. Phys. Rev. E 71:031907.

Hartl, D. L., and C. H. Taubes. 1998. Towards a theory of evolutionary adaptation. Genetica 103:525–533.

Hietpas, R. T., C. Bank, J. D. Jensen, and D. N. A. Bolon. 2013. Shifting fitness landscapes in response to altered environments. Evolution 67: 3512–3522.

Immler, S., G. Arnqvist, and S. P. Otto. 2012. Ploidally antagonistic selection maintains stable genetic polymorphism. Evolution 66:55–65.

Innocenti, P., and E. H. Morrow. 2010. The sexually antagonistic genes of *Drosophila melanogaster*. PLoS Biol. 8:e1000335.

Jasmin, J. N., and C. Zeyl. 2013. Evolution of pleiotropic costs in experimental populations. J. Evol. Biol. 26:1363–1369.

Jasnos, L., K. Tomala, D. Paczesniak, and R. Korona. 2008. Interactions between stressful environment and gene deletions alleviate the expected average loss of fitness in yeast. Genetics 178:2105–2111.

Kassen, R. 2002. The experimental evolution of specialists, generalists, and the maintenance of diversity. J. Evol. Biol. 15:173–190.

Kassen, R., and T. Bataillon. 2006. Distribution of fitness effects among beneficial mutations before selection in experimental populations of bacteria. Nat. Genet. 38:484–488.

Kirkpatrick, M., and N. H. Barton. 1997. Evolution of a species' range. Am. Nat. 150:1–23.

Kopp, M., and S. Matuszewski. 2014. Rapid evolution of quantitative traits: theoretical perspectives. Evol. Appl. 7:169–191.

Korona, R. 2004. Experimental studies of deleterious mutation in *Saccharomyces cerevisiae*. Res. Microbiol. 155:301–310.

Lalic, J., J. M. Cuevas, and S. F. Elena. 2011. Effect of host species on the distribution of mutational fitness effects for an RNA virus. Plos Genet. 7:7.

Lande, R. 1980. The genetic covariance between characters maintained by pleiotropic mutations. Genetics 94:203–215.

Lenormand, T. 2012. From local adaptation to speciation: specialization and reinforcement. Int. J. Ecol. 2012:11.

Lenormand, T., and M. Raymond. 1998. Resistance management: the stable zone strategy. Proc. R Soc. Lond. B 265:1985–1990.

Levins, R. 1968. Evolution in changing environments. Princeton Univ. Press, Princeton.

MacLean, R. C., G. G. Perron, and A. Gardner. 2010. Diminishing returns from beneficial mutations and pervasive epistasis shape the fitness landscape for rifampicin resistance in *Pseudomonas aeruginosa*. Genetics 186:1345–1354.

Martin, G. 2014. Fisher's geometrical model emerges as a property of large integrated phenotypic networks. Genetics 197:237–255.

Martin, G., S. F. Elena, and T. Lenormand. 2007. Distributions of epistasis in microbes fit predictions from a fitness landscape model. Nat. Genet. 39:555–560.

Martin, G., and T. Lenormand. 2006a. The fitness effect of mutations across environments: a survey in light of fitness landscape models. Evolution 60:2413–2427.

Martin, G., and T. Lenormand. 2006b. A general multivariate extension of Fisher's geometrical model and the distribution of mutation fitness effects across species. Evolution 60:893–907.

McCandlish, D. M., C. L. Epstein, and J. B. Plotkin. 2014. The inevitability of unconditionally deleterious substitutions during adaptation. Evolution 68:1351–1364.

McCandlish, D. M., and A. Stoltzfus. 2014. Modeling evolution using the probability of fixation: history and implications. Quart. Rev. Biol. 89:225–252.

Moorad, J. A., and D. W. Hall. 2009. Age-dependent mutational effects curtail the evolution of senescence by antagonistic pleiotropy. J. Evol. Biol. 22:2409–2419.

Nagylaki, T. 1980. The strong-migration limit in geographically structured populations. J. Math. Biol. 9:101–114.

Orr, H. A. 1998. The population genetics of adaptation: The distribution of factors fixed during adaptive evolution. Evolution 52:935–949.

Orr, H. A. 2000. Adaptation and the cost of complexity. Evolution 54:13–20.

Orr, H. A. 2005. The genetic theory of adaptation: a brief history. Nat. Rev. Genet. 6:119–127.

Ostrowski, E. A., D. E. Rozen, and R. E. Lenski. 2005. Pleiotropic effects of beneficial mutations in *Escherichia coli*. Evolution 59:2343–2352.

Perfeito, L., A. Sousa, T. Bataillon, and I. Gordo. 2014. Rates of fitness decline and rebound suggest pervasive epistasis. Evolution 68:150–162.

Polechova, J., N. Barton, and G. Marion. 2009. Species' range: adaptation in space and time. Am. Nat. 174:E186–E204.

Poon, A., and S. P. Otto. 2000. Compensating for our load of mutations: freezing the meltdown of small populations. Evolution 54:1467–1479.

Remold, S. K., and R. E. Lenski. 2001. Contribution of individual random mutations to genotype-by-environment interactions in *Echerichia coli*. Proc. Natl. Acad. Sci. 98:11388–11393.

Rice, S. H. 1990. A geometric model for the evolution of development. J. Theoret. Biol. 143:319–342.

Rice, S. H. 2004. Evolutionary theory: mathematical and conceptual foundations. Sinauer Associates, Sunderland, MA.

Roff, D. A., and D. J. Fairbairn. 2007. The evolution of trade-offs: where are we? J. Evol. Biol. 20:433–447.

Ronce, O., and I. Olivieri. 1997. Evolution of reproductive effort in a metapopulation with local extinctions and ecological succession. Am. Nat. 150:220–249.

Slatkin, M. 1978. Spatial patterns in the distributions of polygenic characters. J. Theoret. Biol. 70:213–228.

Sousa, A., S. Magalhaes, and I. Gordo. 2011. Cost of antibiotic resistance and the geometry of adaptation. Mol. Biol. Evol. 29:1417–1428.

Trindade, S., A. Sousa, and I. Gordo. 2012. Antibiotic resistance and stress in the light of Fisher's model. Evolution 66:3815–3824.

Vale, P. F., M. Choisy, R. Froissart, R. Sanjuan, and S. Gandon. 2012. The distribution of mutational fitness effects of phage phi X174 on different hosts. Evolution 66:3495–3507.

Via, S., and R. Lande. 1985. Genotype-environment interaction and the evolution of phenotypic plasticity. Evolution 39:505–522.

Wang, A. D., N. P. Sharp, C. C. Spencer, K. Tedman-Aucoin, and A. F. Agrawal. 2009. Selection, epistasis, and parent-of-origin effects on deleterious mutations across environments in *Drosophila melanogaster*. Am. Nat. 174:863–874.

Welch, J. J., and D. Waxman. 2003. Modularity and the cost of complexity. Evolution 57:1723–1734.

Whitlock, M. C., and R. Gomulkiewicz. 2005. Probability of fixation in a heterogeneous environment. Genetics 171:1407–1417.

Williams, G. C. 1957. Pleiotropy, natural-selection, and the evolution of senescence. Evolution 11:398–411.

Wolfram Research, I. 2012. Mathematica edition: version 9.0. Wolfram Research, Inc., Champaign, Illinois.

Wong, A., N. Rodrigue, and R. Kassen. 2012. Genomics of adaptation during experimental evolution of the opportunistic pathogen *Pseudomonas aeruginosa*. Plos Genet. 8:8.

Yeaman, S., and S. P. Otto. 2011. Establishment and maintenance of adaptive genetic divergence under migration, selection, and drift. Evolution 65:2123–2129.

Associate Editor: D. Hall
Handling Editor: R. Shaw

Supporting Information

Additional Supporting Information may be found in the online version of this article at the publisher's website:

Supplementary Figure 1. geometric derivation of the distribution of (U_i, U_j).
Supplementary Figure 2. bivariate distribution of (U_i, U_j).
Supplementary Figure 3. Robustness of the conditional distribution of $s_j|s_i$.
Supplementary Figure 4A. Bivariate distribution of (S_i, S_j) for various levels of anisotropy.
Supplementary Figure 4B. Environment-independent anisotropy.
Supplementary Figure 5A and B. same as Figure 6 with $\bar{s} = 0.01$and0.1, respectively.